

Tracing neutral gas outflows in [U]LIRGs via optical IFS of the NaD feature

Sara Cazzoli^{1,2}

¹ CSIC, Departamento de Astrofísica-Centro de Astrobiología (CSIC-INTA), Madrid, Spain

² Cavendish Laboratory, University of Cambridge 19 J. J. Thomson Avenue, Cambridge CB3 0HE, UK

Abstract

We describe the results recently obtained for the LIRG IRAS F11506-3851 [6], for which we have detected the presence for a strong neutral gas outflow via NaD 5890, 5896 Å lines using optical VLT VIMOS-IFU observations. The analysis of the geometry of the outflow and of the 2D ongoing SF, indicate a large mass loading factor associated to the nuclear region, suggesting that we are witnessing the quenching of star formation due to SNe feedback. We also present preliminary results for a sample of 38 local [U]LIRGs [7]. We find complex velocity fields and velocity dispersion maps associated to the ISM neutral gas showing that part of it is entraining in starburst driven outflows able to provide a negative feedback on the host galaxy.

1 Introduction

Galactic winds (GWs) regulate and quench both the star formation and the black hole activity, being also the primary mechanism by which dust and metals are redistributed in the interstellar medium (ISM), or even expelled outside the galaxy into the intergalactic medium (IGM; [17]). Cosmological models of galaxy evolution require energetic outflows to reproduce the observed properties of galaxies – i.e., without a strong (stellar or AGN) feedback, they lead galaxies to have much higher star forming rates (SFRs) and larger stellar masses than observed [10].

GWs are ubiquitous at any redshift. Local luminous and ultra-luminous infrared galaxies [U]LIRGs¹ offer the opportunity to study the outflow phenomenon at environments similar to that observed at high- z , but with a much higher S/N and spatial resolution [3, 2].

Of particular interest is measuring the mass of gas being expelled by the wind in its cold

¹LIRGs: $L_{\text{IR}} \equiv L_{(8-1000\mu\text{m})} = 10^{11-10^{12}} L_{\odot}$, ULIRGs: $L_{\text{IR}} \geq 10^{12} L_{\odot}$.

phases (e.g., neutral) since the evacuation of this gas may be responsible for quenching the star formation. The cold neutral gas in winds is detected through absorption features as the sodium doublet, NaD $\lambda\lambda 5890, 5896$ (e.g., [9]). Works using IFS technique has been recently expanded to study the multi-phase structure of outflows, mainly focused in the most luminous merger systems (e.g., [15]) showing that in these objects outflows are massive enough to provide negative feedback to star formation. The neutral outflows in the potentially interesting LIRG range have been not explored in detail (but see [11]).

2 Sample, analysis techniques and 2D maps

We systematic search for neutral gas winds in a sample of 38 nearby [U]LIRGs included in the [U]LIRGs-VIMOS survey [1]. In Section 3 we present the IFS study for the LIRG F11506-3851 ([6], hereafter C14), while preliminary results of our search of neutral winds will be presented in Section 4 and in a forthcoming paper [7]. We choose F11506-3851 as a pilot study, since the availability of both optical VIMOS and near-IR SINFONI IFS-data that allows to simultaneously trace different galaxy components (ISM and stars). Details about these optical-VIMOS and the near-IR SINFONI observations are given in [14] (and references therein) and [13], respectively.

For the LIRG F11506-385, the NaD and the $H\alpha$ -[NII] emission-line complex profiles were modeled with two kinematic components (i.e., a couple Gaussians per line, Fig. 1 left and centre) on spaxel-by-spaxel basis. The output of the fitting (line flux, central wavelength and intrinsic width) were used to generate spectral maps (Fig. 2). The NaD absorption has three contributors at different locations along the line of sight. Specifically, the main NaD component consists of neutral ISM clouds likely forming an irregular disk-like structure and a galactic wind emerging perpendicular to this disk, while the secondary NaD component is likely associated with the stars (Fig. 2, top). In contrast, the main (narrow) component of $H\alpha$ emission probes the ionized gas systemic rotational motions, and the secondary (broad) component seems associated with radial motions (Fig. 2, center). To obtain the stellar kinematic, we studied the near-IR CO(2-0) $\lambda 2.293 \mu\text{m}$ and CO(3-1) $\lambda 2.322 \mu\text{m}$ absorption bands by using the SINFONI observations in the K band (1.95–2.45 μm). We first binned the data using the adaptive Voronoi 2D-binning method [5] and then we used the Penalized PiXel-Fitting method (pPXF; [4]), to fit a library of stellar templates [18] to individual spectra (Fig. 1, right) to create the spectral maps (Fig. 2, bottom).

3 Spatially resolved kinematics, galactic wind, and quenching of star formation in the luminous infrared galaxy IRAS F11506-3851

3.1 Kinematics and dynamical support for the stars and gas phases

The velocity fields of the ionized gas and stars, as traced by the $H\alpha$ (narrow component) and the CO(2-0) line (Fig. 2), present velocity patterns consistent with large, kiloparsec-scale ordered rotational motions. As expected in case of a rotating disk, the $H\alpha$ velocity dispersion

map shows a centrally peaked pattern with its maximum value (i.e., $\sigma_c(\text{H}\alpha) = 95 \pm 4 \text{ km s}^{-1}$). Similarly to the ionized gas, the stars exhibit a centrally peaked velocity dispersion map (Fig. 2), but the nuclear ($R < 0.3 \text{ kpc}$) velocity dispersion is slightly larger than that of the ionized gas (i.e., $136 \pm 20 \text{ km s}^{-1}$). We found that the stars and the ionized gas nearly co-rotate. Their kinematics are consistent with the picture of a (mainly) rotationally supported ionized gas disk embedded in a thicker and dynamically hotter stellar disk (C14). The ionized gas shows a relatively high turbulence compared with normal spirals of lower SFR, but it is not as high as that found at high- z [8].

3.2 Neutral gas kinematics, outflow and feedback

The NaD-EW map suggests a rather irregular and complex distribution of the neutral gas. Excluding a region of strong blueshifted velocities along the semi-minor axis, the overall neutral gas kinematics can be interpreted as a slow rotating disk that lags in velocity to those of the ionized gas and stars, and it is dominated by random motions as indicated by the small V/σ value (i.e., ~ 1). Therefore, part of the neutral gas is distributed in a thick and dynamically hot disk, in contrast to the stars and the ionized gas, which are confined to disks mainly supported by rotation.

Our IFS data show evidence of a conical outflow emerging from the nuclear region perpendicular to the disk at mean velocities of $\sim 100 \text{ km s}^{-1}$. In addition, there is evidence of the presence of an ionized outflow that partially overlaps the wind detected in NaD (C14). In order to estimate the mass loss rate and the mass loading factor of the wind, we apply a thin-shell free wind model [15], considering that the mass outflow rate and the velocities are independent of radius. We have inferred an outflowing mass rate of about $48 M_{\odot} \text{ yr}^{-1}$, which considering the total SFR of this galaxy (i.e., 34) implies a global mass loading factor ($\eta = M_{\odot}/\text{SFR}$) of 1.4. On the basis of the measured outflowing velocities and the galaxy escape velocity, it is unlikely that a significant fraction of the outflowing material would escape the galaxy to chemically enrich the surrounding IGM. Therefore, the outflowing material will fall back onto the galaxy disk, which would explain the lagging and the thickening of the neutral gas disk.

The nuclear region has been identified as the site where the outflow originates. The large local mass loading factor (> 1) associated with this region, together with its relatively modest ongoing SF (seen via $\text{H}\alpha$ emission) and the evidence of SNe (i.e., [FeII] emission, [13]), suggest that the outflow has been generated by the effects of these SNe and it has effectively quenched star formation over the past few Myr in this region. However, the large nuclear reservoir of cold molecular gas, as inferred from the H_2 1-0 S(1) emission [13], suggests that recurrent episodes of SF may occur again.

4 Preliminary results of a search for neutral GWs in the [U]LIRGs-IFS survey

Based on the results of the line-modeling of the NaD absorption doublet (Section 1), within the sample we found conical and collimated extra-planar neutral GWs in the almost half of

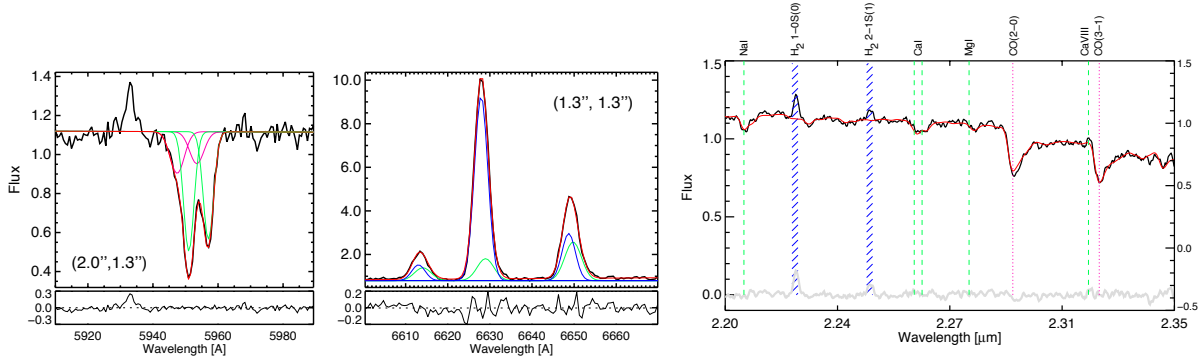


Figure 1: From left to the right: the NaD (*left*) and H α -[NII] (*center*) spectra for selected regions. *Right*: the near-IR spectrum (black) from the central bin (with S/N ~ 27) of IRAS F11506-385. In the labels the coordinates have been indicated as the distance from the nucleus (map center, Fig. 2). For each spaxel the modeled line profile (red line) and the single components (with different colours) are shown, along with the residuals (left and center panels). The green lines represent, respectively, the main-NaD and the narrow-H α Gaussian functions. The stellar-NaD and the broad(outflowing) H α curves are shown in magenta and blue. On the near-IR spectrum (right) is overlaid its best-fitting spectrum derived with the pPXF approach (Section ??) is shown (red line; fit residuals are shown in gray). The wavelength regions excluded during the fitting are marked in dark blue. The most relevant spectral features are labeled at the top and marked with a dashed green line, while the CO bands are marked with a magenta dotted-point line.

the sample (i.e., 23/51). Among these, for 6 galaxies, the GWs are not clearly detected. Interestingly, the quoted occurrence of outflows in the galaxies of our sample is not related to the gas content or to the inclination of the host galaxy [7].

The median velocities of the neutral gas winds with confirmed detection is in the range ~ 100 – 300 km s^{-1} , similar to what was found in previous works (Fig. 3, left). While GWs in 3 galaxies have somewhat larger velocities (~ 300 – 500 km s^{-1}) indicative of powerful starbursts, one galaxy shows outflowing speeds that exceed 1000 km s^{-1} typical of AGN-driven winds. The median velocity dispersion of the observed GWs is in the range ~ 90 – 180 km s^{-1} , therefore larger than the thermal velocity dispersion of the warm neutral gas [17], indicating that these winds are turbulent and associated with shocks.

The quantitative measurements of the feedback (negative, in nearly all the cases) such as mass outflow rate, energy and efficiency are related to the properties of the underlying starburst. Indeed, for example, outflows in LIRGs are less extreme, as expected according to the positive relation within the outflow velocity and SFR [12], Fig. 3, left). This trend is similar to the one found for ionized gas winds in [U]LIRGs [2].

We also find that the starburst is generally the main driver of the outflows, according to the comparison within the wind power and the kinetic power of the starburst associated to the SNe (Fig. 3, right, [7]).

References

- [1] Arribas S., Colina L., Monreal-Ibero A., et al. 2008, A&A, 479, 687
- [2] Arribas, S., Colina, L., Bellocchi, E., arXiv:1404.1082
- [3] Bellocchi E., Arribas, S., Colina L. 2013, A&A 557, 59

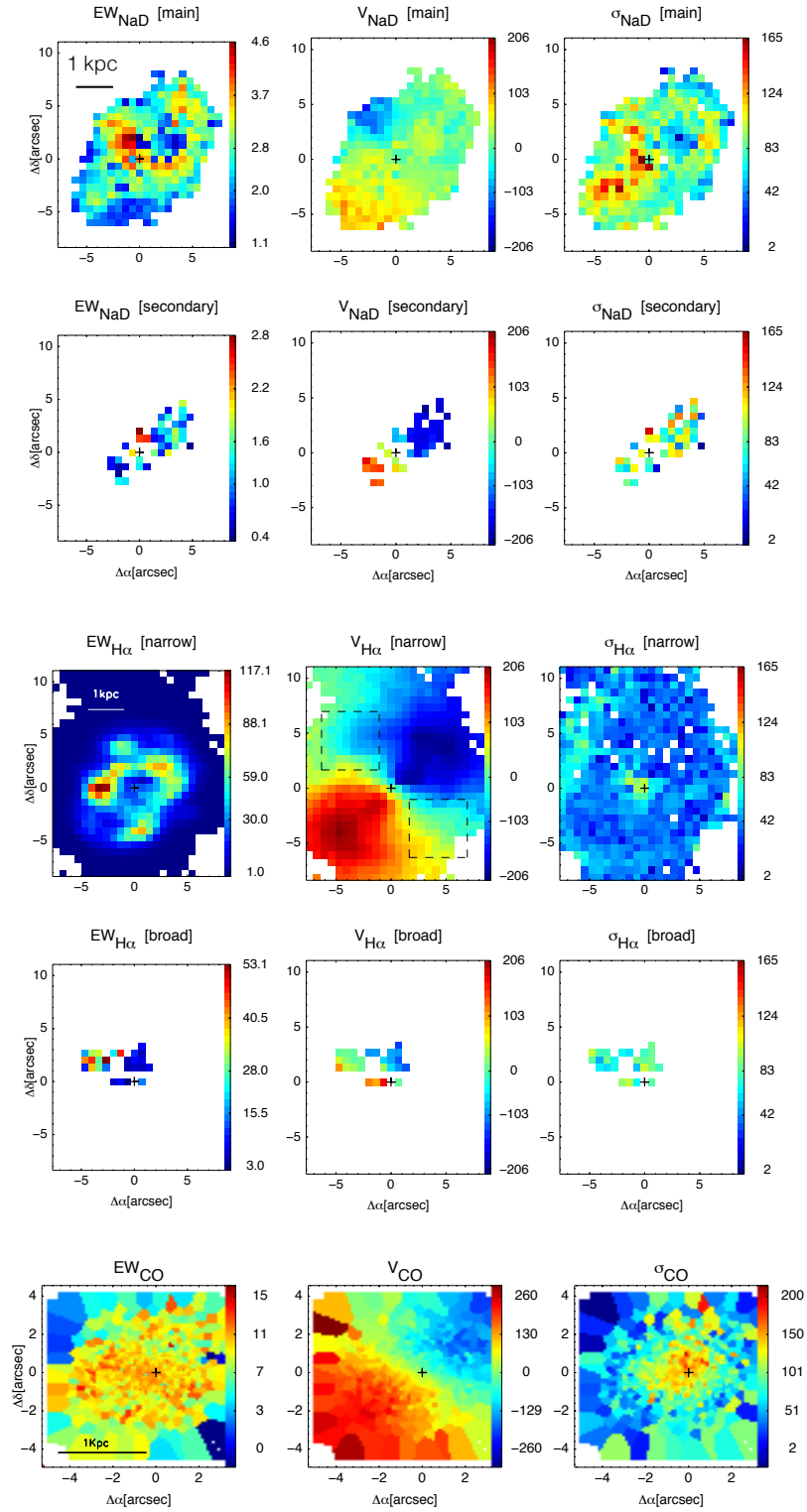


Figure 2: From left to the right equivalent width, velocity and velocity dispersion maps of different kinematic components of the NaD (top) and H α (centre) line profiles. In the lower panel, the SINFONI maps of the CO(2-0) IR absorption line are also presented. The equivalent width maps are given in \AA units and, while, the velocity and velocity dispersion maps are in km s^{-1} units. Crosses mark the optical and near-IR nuclei. The boxes in the central panel indicates the region where a search for an ionized wind has been accomplished.

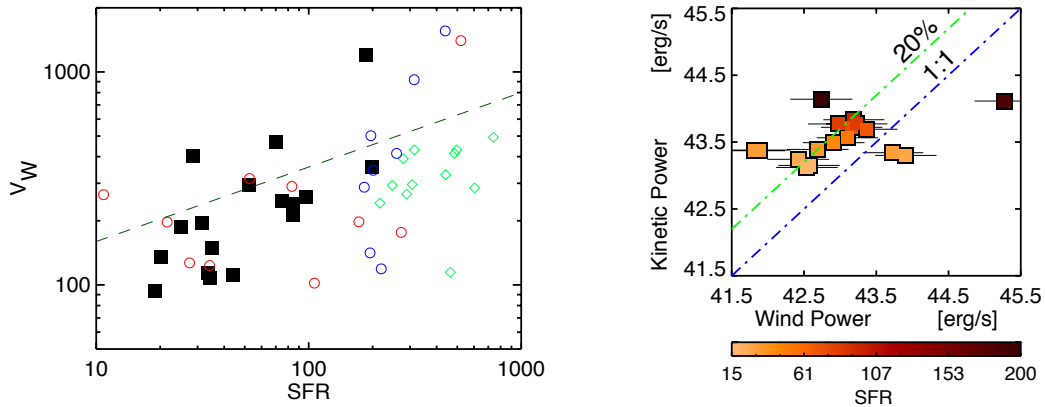


Figure 3: *Left*: V -SFR relation and the comparison of our data (black) with the literature ([15]: LIRGs and ULIRGs, blue and red, respectively and green diamonds [12]. *Right*: kinetic power of the starburst associated to SNe as a function of the wind kinetic power (color coded by SFR). Blue and green line represent the 1:1 correlation and its 20%.

- [4] Cappellari, M. & Copin, Y. 2003, MNRAS, 342, 345
- [5] Cappellari M., & Emsellem E. 2004, PASP, 116, 138
- [6] Cazzoli S., Arribas S., and Colina L., et al. 2014, arXiv:1406.5154
- [7] Cazzoli S., Arribas S., and Maiolino R., et al. 2015, in prep.
- [8] Förster Schreiber N.M., Shapley A.E., Genzel R., et al., 2011, ApJ, 739:45
- [9] Heckman T. Lehnert, M. D. Strickland D. K., & Lee A. 2000, ApJS, 129, 493
- [10] Hopkins P.F., Quataert E. and Murray N., 2012, MNRAS, 421:3522-3537, 2012
- [11] Jiménez-Vicente, J., Castillo-Morales A., Mediavilla E., et al. 2007, MNRAS, 382, L16
- [12] Martin, C. L. 2005, ApJ, 621:227 - 245
- [13] Piqueras López, J., Colina L., Arribas S., et al. 2012, A&A, 546, 64
- [14] Rodríguez-Zaurín, J., Arribas, S., Monreal-Ibero, A., et al. 2011, A&A, 527, A60
- [15] Rupke D. S., Veilleux, S. & Sanders D. B. 2005, ApJS, 160, 115
- [16] Rupke D. S., & Veilleux S., 2013, ApJ, 768, 75
- [17] Veilleux, S., Cecil, G. & Bland-Hawthorn J. 2005, ARA&A, 43, 769
- [18] Winge C., Riffel R. A., & Storchi-Bergmann T. 2009, ApJS, 185, 186